FIRE AND MATERIALS
Fire Mater. 2006; **30**:311–321
Published online 3 October 2005 in Wiley InterScience (www.interscience.wiley.com). DOI: 10.1002/fam.916

Towards a methodology for the characterization of fire resistive materials with respect to thermal performance models[‡]

Dale P. Bentz[*,†], Kuldeep R. Prasad and Jiann C. Yang

Building and Fire Research Laboratory, National Institute of Standards and Technology, Gaithersburg, MD 20899-8615, U.S.A.

SUMMARY

A methodology is proposed for the characterization of fire resistive materials with respect to thermal performance models. Typically in these models, materials are characterized by their densities, heat capacities, thermal conductivities, and any enthalpies (of reaction or phase changes). For true performance modelling, these thermophysical properties need to be determined as a function of temperature for a wide temperature range from room temperature to over 1000°C. Here, a combined experimental/theoretical/modelling approach is proposed for providing these critical input parameters. Particularly, the relationship between the three-dimensional microstructure of the fire resistive materials and their thermal conductivities is highlighted. Published in 2005 by John Wiley & Sons, Ltd.

KEY WORDS: density; enthalpy; fire resistive materials; heat capacity; microstructure; thermal conductivity

INTRODUCTION

As progress is made in the integration of structural and fire performance models for structural steel, one key component is a proper and accurate characterization of the thermophysical properties of the fire resistive materials (FRM). To predict the surface temperatures of the steel and its subsequent mechanical performance, an understanding of the energy transfer from the fire to the steel through the FRM is paramount. The four major thermophysical properties needed to model the thermal performance of the FRMs are: density, heat capacity, thermal conductivity, and enthalpy (of reactions and phase changes). Furthermore, these properties are needed as a function of temperature, from room temperature to temperatures greater than 1000°C. In this paper, various approaches for obtaining these data are reviewed and critiqued. It appears that a combination of experimental measurements and theoretical/modelling computations will provide the most robust and accurate characterization for these materials. While the mechanical integrity and adhesion properties of the FRMs as a function of temperature are also critical to successful performance during a fire exposure, they will not be considered in this initial study.

[*]Correspondence to: Dale. P. Bentz, Building and Fire Research Laboratory, National Institute of Standards and Technology, Gaithersburg, MD 20899-8615, U.S.A.
[†]E-mail: dale.bentz@nist.gov

Received 1 August 2004
Revised 15 August 2005
Accepted 16 August 2005

MATERIALS

Representative samples of four spray-applied FRMs were obtained from two of the largest manufacturers in the industry. Two of the materials are mainly composed of mineral fibres with a portland-cement-based binder. The other two are gypsum-based with either vermiculite or expanded polystyrene beads as lightweight extenders. In the sections that follow, the materials will be identified only by their binder components, portland cement and gypsum, respectively. Two of the materials (one portland-cement-based and one gypsum-based) are currently available in the U.S. marketplace, while the other two were of interest for historical reasons and are still in use in various existing structures. In the latter case, the materials were supplied by the manufacturers in a condition that matched the historical materials as closely as possible. Samples of both of the portland-cement-based and one of the gypsum-based materials were sent to a commercial testing laboratory for evaluation of thermal conductivity, heat capacity, and density (via mass and thermal expansion measurements) [1]. In addition, the materials were characterized by thermogravimetric, dimensional, differential scanning calorimetry, and optical microscopy analysis in the NIST labs.

PROPERTIES

Density

The two contributions to the density of any material are its mass and its volume. FRMs are complex in that both of these contributions are changing during a fire exposure. As exemplified in Figures 1 and 2, most FRMs will lose mass in a monotonic fashion during a high temperature or fire exposure, due to some combination of dehydration, decarbonation, and decomposition of organic compounds. Their volume, however, may either increase or decrease. An increase in volume may be observed as the solid network supporting the FRM expands with increasing temperature or more dramatically when an intumescent coating foams during thermal degradation. A decrease in volume may be observed as shrinkage accompanies the mass loss from this solid network.

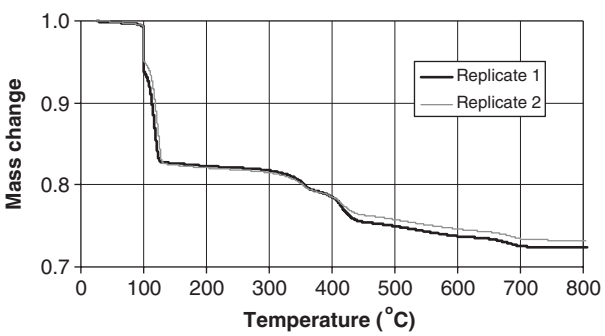

Figure 1. Example thermogravimetric results for a gypsum-based spray-applied FRM with a nominal heating rate of 5°C/min. Results are for two nominally identical ≈ 50 mg replicates. Maximum observed coefficient of variation (COV) for mass loss between the two replicate samples is 0.9%.

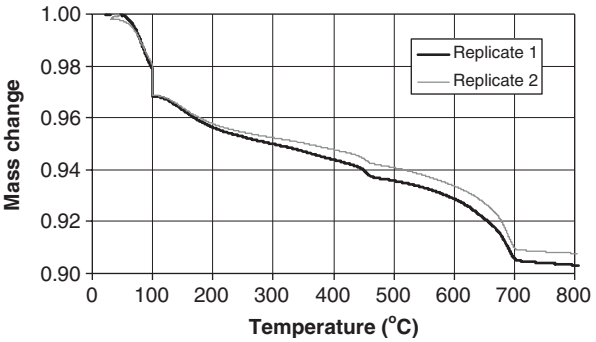

Figure 2. Example thermogravimetric results for a portland-cement-based spray-applied FRM with a heating rate of 5°C/min. Results are given for two nominally identical ≈ 50 mg replicates. Maximum observed COV for mass loss between the two replicate samples is 0.4%.

Mass loss can be quantified using thermogravimetric analysis (TGA), as described in ASTM E1131 [2]. Of course, the results will vary with the programmed heating rate, sample size, and sample environment. As shown in Figure 1, spray-applied FRMs may lose as much as 25% of their initial mass during exposure to 800°C. This mass loss also provides critical input for calculating the enthalpies of reaction for the in-place FRM. Once a set of reactions is hypothesized, the standard heats of reactions may be calculated and normalized by the measured mass loss to calculate the enthalpy change for the in-place material, as will be demonstrated later in this paper.

Volume changes (thermal expansion) can be measured using a dilatometer (ASTM E228) or interferometry (ASTM E289) [2]. High temperature measurements (e.g. >600°C) are often complicated by the large dimensional changes that may be experienced in FRMs, along with their generally fragile nature. In addition, spray-applied materials are inherently anisotropic and may thus exhibit different coefficients of thermal expansion in the in-plane and through-thickness dimensions.

Typically, the density at any given temperature is calculated as the ratio of the measured mass at that temperature to the measured volume at that temperature.

Heat capacity

Two common approaches to estimating heat capacity are as follows: (1) calculate C_p from a measurement of thermal diffusivity and knowledge of the density and thermal conductivity of the FRM, or (2) measure C_p directly using a differential scanning calorimeter (DSC). The former is often complicated by the dynamic nature of FRMs, as they typically lose significant mass during the measurement time. An exciting recent development for the latter method is the availability of commercial simultaneous thermal analysis (STA) units. These units permit the simultaneous monitoring of heat flow and mass during exposure to a (high) temperature regime. With conventional DSC, only the heat flow is measured and to obtain the specific heat per unit mass of material that is the required input for thermal performance models, the results need to be adjusted by mass measurements (TGA) made on a companion sample. The advantages of making both measurements simultaneously on the same material

specimen are obvious. In addition, newer commercial STA units may allow for larger sample volumes/masses (on the order of 1 g as opposed to the 50–100 mg typical of most DSCs). This is especially important for typical spray-applied FRMs that may exhibit a microstructural heterogeneity on the scale of millimeters. For some fire resistive materials, such as concrete, even a 1 g sample size is likely to be insufficient to provide a representative sample volume. For FRMs whose mass composition is exactly known, an alternative approach is to calculate the FRM heat capacity as a mass-weighted average of the heat capacities of the component materials. Of course, this requires that C_p data as a function of temperature are available for each component.

To obtain quantitative C_p data (via ASTM E1269 for example [2]), the typical procedure is to use a sapphire or other reference specimen to obtain a correction factor (graciously named the 'calorimetric sensitivity' in the ASTM E1269 standard) under the same operating conditions as those used for the test specimen. Due to typical mass mismatch between the reference and sample pans, further corrections may be needed based on the known tabulated heat capacities of aluminium or gold (pans) as a function of temperature. A typical set of DSC curves for a spray-applied FRM are provided in Figure 3. The presence of several endothermic peaks is clearly indicated. The binder component of this particular FRM is portland-cement-based and the first two peaks (at about 65 and 110°C) correspond to the loss of bulk (free) water and (loosely) bound water from gel-like hydration products, respectively, the third peak (near 420°C) to the loss of chemically bound water from calcium hydroxide, and the fourth peak (near 650°C) most likely to the loss of carbon dioxide from carbonated reaction products. This material exhibited about a 10% mass loss during exposure up to 700°C, so that the correction for the variable mass of the specimen during the test was only of minor significance. By integrating the area under these peaks, the corresponding enthalpies of reaction could be estimated. However, with the small sample size employed in this experiment (<10 mg), a quantitative interpretation is hindered by the previously mentioned heterogeneity of the material, e.g. most likely a representative volume was not sampled in this specific DSC measurement.

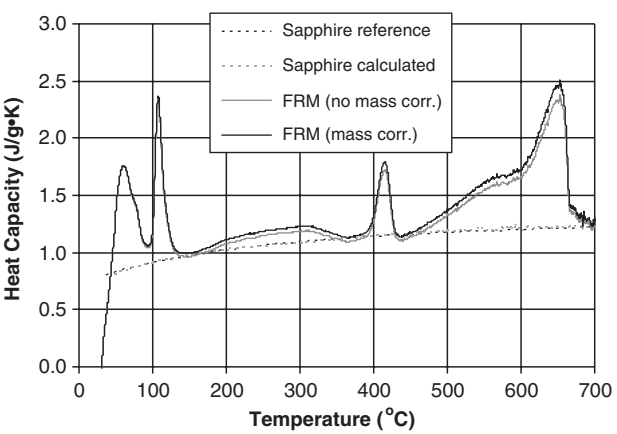

Figure 3. Example DSC results (original and mass corrected) for a portland-cement-based spray-applied FRM using gold pans and a sapphire reference.

Table I. Thermophysical properties for gypsum-based compounds at 25°C [3, 4].

Compound	Molar mass (g/mol)	C_p (J/mol °C)	H_f (kJ/mol)
Gypsum ($CaSO_4-2H_2O$)	172.2	186.2	−2024
Hemihydrate ($CaSO_4-0.5H_2O$)	145.2	119.5	−1578
Anhydrite ($CaSO_4$)	136.1	99.7	−1435
H_2O (gas)	18.0	33.6	−242

Enthalpies of reaction

If the chemical composition of the FRM is known, the potential exists to calculate the enthalpies of reaction from heats of formation and heat capacity data [3, 4]. The standard procedure is to 'cool' the reactants down from the reaction temperature to a reference state (temperature) of 25°C, compute the heat of reaction at 25°C, and then heat the products back up to the reaction temperature [4]. Here, we will illustrate this simple procedure for a gypsum-based FRM. Gypsum, which contains two molecules of water for each molecule of calcium sulphate, undergoes two dehydration reactions when exposed to elevated temperatures, first converting to calcium sulphate hemihydrate and then to the anhydrite form of calcium sulphate. The heat capacities and heats of formation (H_f) of the relevant compounds are provided in Table I [3, 4]. Care must be taken to consider water in its gas phase form as the reaction temperatures being considered are always above 100°C. Using these properties and the known dehydration reaction stoichiometries (e.g. $CaSO_4-2H_2O \rightarrow CaSO_4-0.5H_2O + 1.5\ H_2O$ and $CaSO_4-0.5H_2O \rightarrow CaSO_4 + 0.5\ H_2O$), heats of reaction of 3.01 kJ/g water lost at 150°C and 2.35 kJ/g water lost at 250°C are calculated for the dehydrations to hemihydrate and anhydrite, respectively. These values are in reasonable agreement with those recently summarized for gypsum plasterboard by Thomas [5]. These values could then be multiplied by the corresponding measured mass loss in these temperature ranges (from Figure 1 for example) to obtain the enthalpy changes due to reactions for a particular FRM during fire exposure. Similar calculations can be employed for portland-cement-based and intumescent FRMs, as long as their specific decomposition reactions and corresponding thermophysical properties are known [6, 7]. It is worth noting that not all reactions in commercially available FRMs are endothermic in nature, as organic components may provide significant exotherms, further supplementing the energy being provided by a fire.

Thermal conductivity

A wide variety of experimental techniques exist for measuring the thermal conductivity of materials at elevated temperatures: high temperature guarded hot plate (ASTM C177), heat flow meter apparatus (ASTM C518), laser flash diffusivity methods (ASTM E1461), and transient line/hot wire (ASTM C1113) and plane source methods [2, 8–10]. Similar to the discussion presented for concrete by Flynn [8], these measurements are always complicated by the dynamic nature of the FRM which is undergoing degradation even as its thermal conductivity is being measured.

An alternative to measuring the thermal conductivities of FRMs at high temperatures is to measure the value at room temperature (or perhaps up to 100°C) and 'predict' the higher

temperature values based on some theory for the conductivity of composite (porous) materials. For example, theories that are closer to reality than the simplest parallel and series models include those of Russell [11], Frey [12] and Bruggeman [13]. For example, the theory of Russell estimates the thermal conductivity of the porous material, k, as [11]

$$k = k_{\text{solid}} \frac{v p^{2/3} + 1 - p^{2/3}}{v(p^{2/3} - p) + 1 - p^{2/3} + p} \tag{1}$$

where $v = k_{\text{gas}}/k_{\text{solid}}$, k_{solid} = thermal conductivity of solid material, p = porosity = $(\rho_{\max} - \rho_{\text{matl}})/\rho_{\max}$, $\rho_{\max}$ = density of solid material in the porous system, ρ_{matl} = density of the porous material, and k_{gas} = thermal conductivity of gas = $k_{\text{cond}} + k_{\text{rad}}$.

For a spherical pore of radius r, the radiation contribution to the overall thermal conductivity of the pore is [14]

$$k_{\text{rad}} = \tfrac{16}{3} r \sigma E T^3 \tag{2}$$

with σ= Stefan–Boltzmann constant ($5.669 \times 10^{-8}\,\text{W/m}^2\,\text{K}^4$), E= emissivity of solid material (1.0 for black bodies), and T = absolute temperature (K).

Knowing the densities of the FRM and the base solid components (by grinding to a powder and measuring in an alcohol solution, for instance), one can calculate the porosity of the FRM. This, along with estimates of the solid's thermal conductivity and the material's typical pore radius, and the tabulated thermal conductivity of air as a function of temperature [3, 15] permits the estimation of the thermal conductivity of the FRM at elevated temperatures. As shown in Figures 4 and 5, application of this theory to both portland-cement-based and gypsum-based spray-applied FRMs yields results in good agreement with existing measurements. While the measured values of $\rho_{\max}$ and ρ_{matl} were used in the calculations, in each case, the pore radius was a floating parameter that was adjusted to give a reasonable fit to the experimental data. But, in each case, the adjusted value for the pore radius is in agreement with visual optical microscopy observations of the characteristic pore sizes in these materials (Figures 6–8). These figures illustrate the potential of applying this approach *in lieu* of or to minimize the number of complicated and costly high temperature measurements for these materials. The approach also points out the advantage of incorporating smaller pores into the FRM structure, as the insulating performance of materials with larger ones will suffer significantly due to radiation effects at higher temperatures.

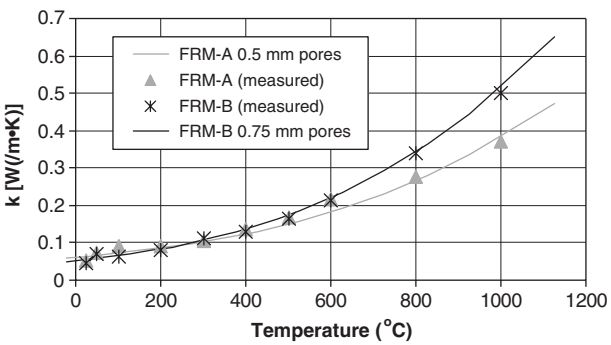

Figure 4. Measured thermal conductivities [1] and predictions based on theory of Russell/Loeb [11, 14] for two similar portland-cement based spray-applied FRMs.

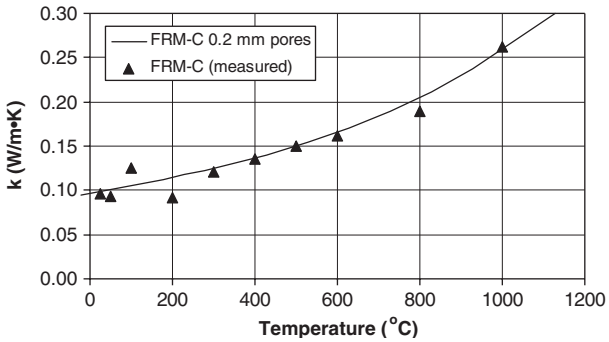

Figure 5. Measured thermal conductivities [1] and predictions based on theory of Russell/Loeb [11, 14] for a gypsum-based spray-applied FRM.

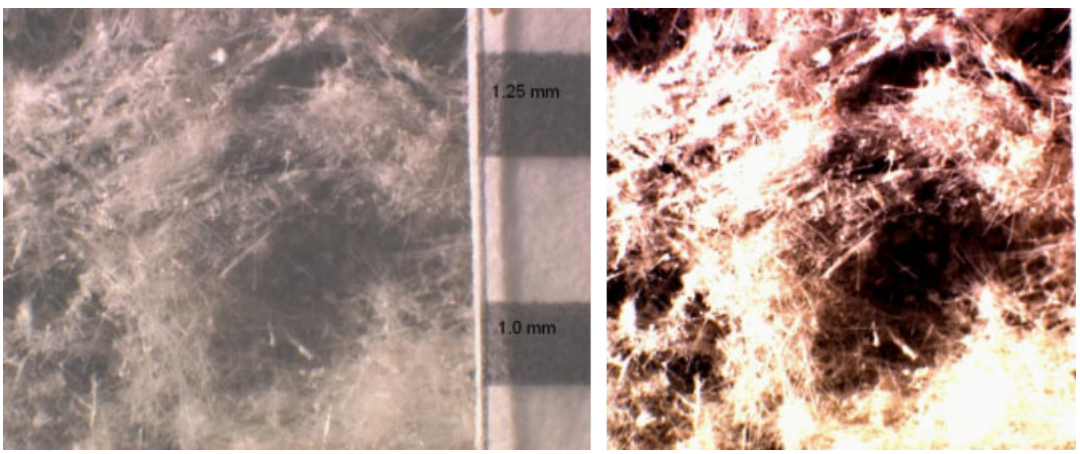

Figure 6. Optical micrograph for portland-cement-based spray-applied FRM-A. Typical pore *diameter* as indicated by the labelled scale bars in the middle of the two images is on the order of 1.0 mm corresponding to a pore radius of 0.5 mm. The original image is on the left and a contrast-enhanced version that better highlights the porosity is shown on the right.

Successful application of this theory requires a detailed understanding of the dynamic microstructure of the FRM. For example, one widely used spray-applied FRM utilizes expanded polystyrene (EPS) beads as a lightweight aggregate. When these highly porous beads decompose at elevated temperatures, even though the total porosity will not change significantly, a new larger size of characteristic pores will be created within the microstructure, potentially leading to an increase in thermal conductivity. Intumescents will also be a challenging application, as in this case, the pore size and total porosity are both dynamic variables that change dramatically during the fire exposure and charring of the coating.

A more detailed microstructural analysis is possible via the utilization of X-ray microtomography which can capture the three-dimensional microstructure of materials with a voxel dimension on the order of micrometers [16]. For example, two-dimensional images (slices) obtained for both gypsum-based and portland-cement-based FRMs using one of the X-ray

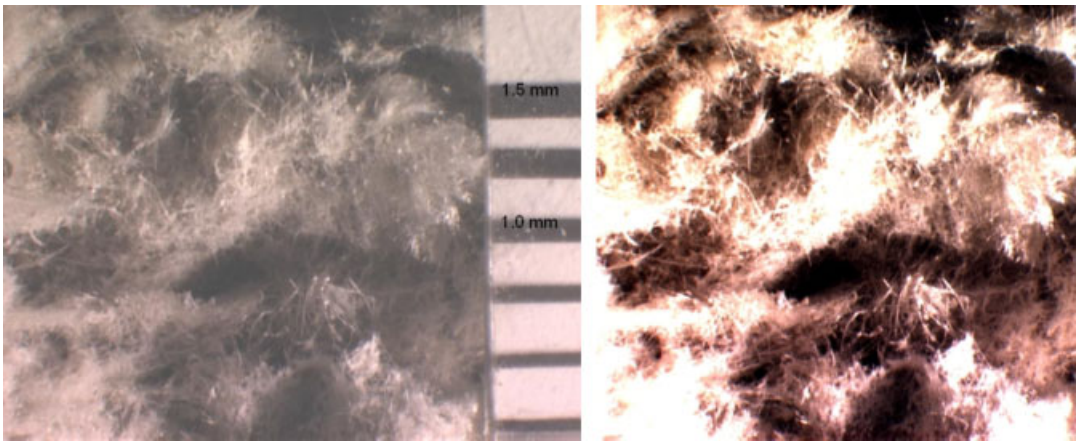

Figure 7. Optical micrograph for portland-cement-based spray-applied FRM-B. Typical pore *diameter* as indicated by the labelled scale bars in the middle of the two images is on the order of 1.5 mm corresponding to a pore radius of 0.75 mm. The original image is on the left and a contrast-enhanced version that better highlights the porosity is shown on the right.

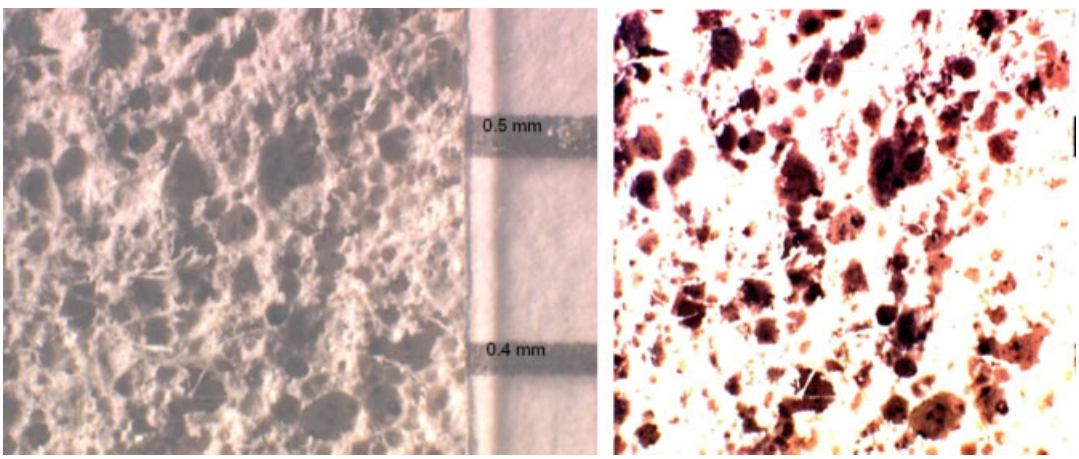

Figure 8. Optical micrograph for gypsum-based spray-applied FRM-C. Typical pore *diameter* as indicated by the labelled scale bars in the middle of the images is on the order of 0.4 mm corresponding to a pore radius of 0.2 mm. The original image is on the left and a contrast-enhanced version that better highlights the porosity is shown on the right.

microtomography units available at the Center for Quantitative Imaging at Pennsylvania State University are provided in Figure 9.[§] These digital image-based three-dimensional microstructures can be segmented into solid and pore phases, and finite element and finite difference

[§] Certain commercial products are identified in this paper to specify the materials used and procedures employed. In no case does such identification imply endorsement by the National Institute of Standards and Technology, nor does it indicate that the products are necessarily the best available for the purpose.

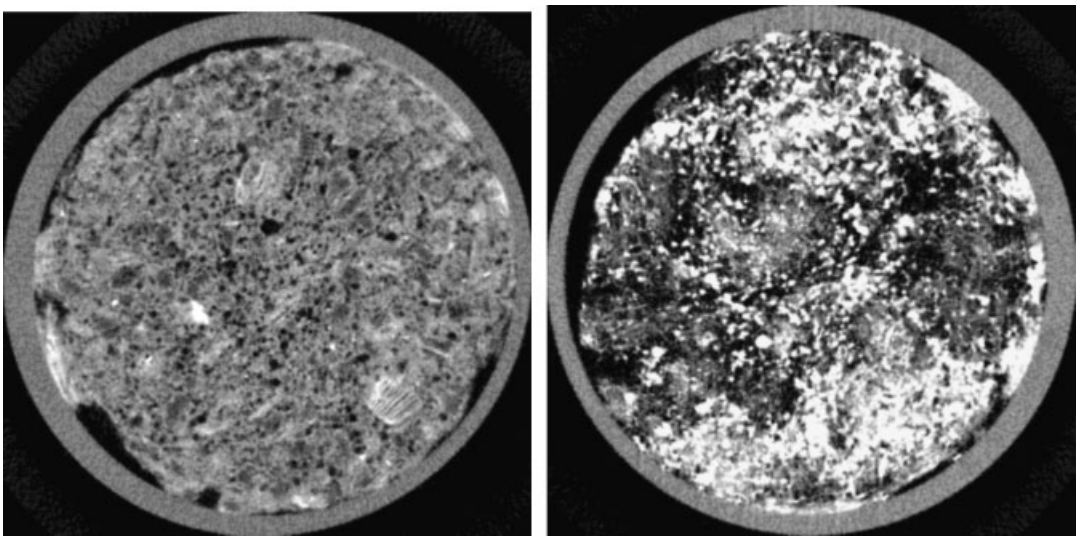

Figure 9. Examples of two-dimensional images from three-dimensional microtomography data sets for gypsum-based (left) and mineral fibre/portland-cement-based (right) FRMs. Materials were imaged in a polypropylene tube with a nominal inner diameter (ID) of 27 mm.

techniques applied to compute their equivalent thermal conductivity [17]. For example, a numerical temperature gradient could be placed across the microstructure and the computed heat flow used to determine the thermal conductivity of the composite 3-D microstructure. Thus, this approach is similar to that used in conventional computational thermal analysis, but it is being applied at the microstructure scale instead of the conventional macro (structure) scale.

RECOMMENDED PROCEDURES

A recommended approach for supplying the thermophysical properties needed by thermal performance models is the following:

(1) Density—determine density via the concurrent measurement of mass and dimensional changes using thermogravimetric and thermal expansion measurements;
(2) Heat capacity—determine heat capacity as a function of temperature using the largest readily available sample cell and a STA unit, and following the ASTM E1269 protocols [2];
(3) Enthalpies of reaction—compute enthalpies based on the mass loss (TGA) measurement and the calculated enthalpies of reaction based on a detailed knowledge of the FRM and its thermal decomposition (these calculations can be critically examined by comparison with analysis of the endotherms and exotherms in the STA results);
(4) Thermal conductivity—supplement direct 'low' temperature thermal conductivity measurements with detailed characterization of the microstructure of the FRM (porosity and pore size) and application of the theory of Russell (or other equivalent) to provide high temperature estimates.

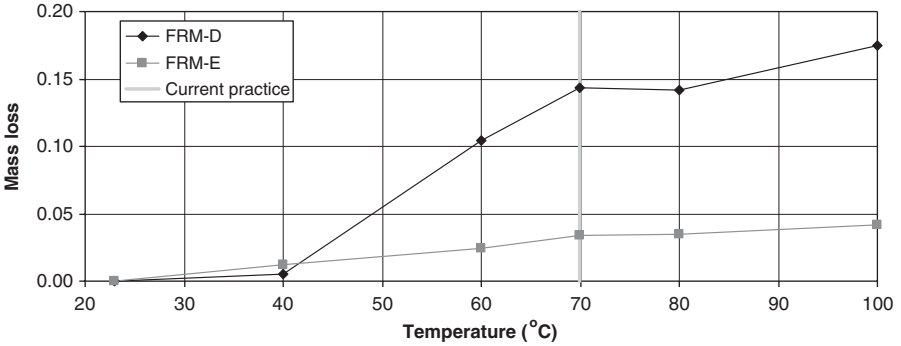

Figure 10. Mass loss (fraction) upon long term (two to three months) oven exposure to different temperatures for gypsum-based (FRM-D) and portland-cement-based (FRM-E) FRMs (sample size of ≈ 3 g).

A WORD OF CAUTION ABOUT AGING TESTS

One of the action items that came out of the initial FEMA study [18] of the collapse of the World Trade Center was that the durability of FRMs is a little-considered but critically important component of their long term performance. In response to this, Underwriters Laboratories, along with the FRM industry and end users, are developing a draft standard to assess the durability of FRMs [19], based on their existing evaluations of intumescent coatings for outdoor use. The basic procedure is to expose the FRM to some aging environment and then verify through thermal exposure (fire) testing that the performance of the aged material is at least equivalent to a specified percentage of that of the original material. Performance is generally assessed in terms of the time that it takes a steel (duct) pipe protected with the FRM to reach a specific temperature (typically 538°C) when exposed to a standard temperature rise curve 'fire environment'. In developing these durability exposures, care must be taken that the exposure conditions are both reasonable and applicable to the various classes of spray-applied FRMs. For example, as shown in Figure 10, the current practice of exposing intumescents to a temperature of 70°C for 270 days can result in considerable mass loss for other types of spray-applied FRMs, even for much shorter exposures of two to three months (particularly those based on gypsum binders). Since the loss of water due to dehydration during a fire exposure is one of the mechanisms by which these materials 'insulate' the steel substrate, it would be expected that these 'aged' materials would exhibit an inferior performance in comparison to their original counterparts. But, is it the material performance or the aging conditions that should be called into question? When moisture is added to the aging exposures, the degradation may become even greater for conventional fibrous insulating materials [20].

ACKNOWLEDGEMENTS

The authors would like to thank Dr Phillip M. Halleck and Dr Abraham S. Grader of the Center for Quantitative Imaging, Pennsylvania State University, for supplying the microtomographic images shown in Figure 9.

REFERENCES

1. Anter Laboratories, Inc. Transmittal of Test Results, *Report to NIST*, 2004.
2. *ASTM Annual Book of Standards*. ASTM International: West Conshohocken, 2004.
3. *CRC Handbook of Chemistry and Physics* (68th edn). CRC Press: Boca Raton, FL, 1987.
4. Smith JM, Van Ness HC. *Introduction to Chemical Engineering Thermodynamics*. McGraw-Hill: New York, 1975.
5. Thomas G. *Fire and Materials* 2002; **26**:37–45.
6. Taylor HFW. *Cement Chemistry*. Thomas Telford: London, 1997.
7. Hansen PF, Hansen J, Hougaard KV, Pedersen EJ. Thermal properties of hardening cement paste. *Proceedings of the RILEM International Conference on Concrete at Early Ages*. RILEM: Paris, 1982; 23–26.
8. Flynn DR. Response of high performance concrete to fire conditions: review of thermal property data and measurement techniques. *NIST GCR 99-767*, U.S. Department of Commerce, March 1999.
9. Gustafsson SE. *Review of Scientific Instruments* 1991; **62**:797–804.
10. Log T, Gustafsson SE. *Fire and Materials* 1995; **19**:43–49.
11. Russell HW. *Journal of the American Ceramic Society* 1935; **18**:1–5.
12. Frey S. *Zeitschrift fur Elektrochemie* 1932; **38**:260–274.
13. Bruggeman DAG. *Annalen der Physik* 1935; **24**:636–664.
14. Loeb AL. *Journal of the American Ceramic Society* 1954; **37**:96–99.
15. Holman JP. *Heat Transfer*. McGraw-Hill: New York, 1981.
16. Bentz DP, Mizell S, Satterfield S, Devaney J, George W, Ketcham P, Graham J, Porterfield J, Quenard D, Vallee F, Sallee H, Boller E, Baruchel J. *Journal of Research of the National Institute of Standards and Technology* 2002; **107**:137–148.
17. Garboczi EJ. Finite element and finite difference programs for computing the linear electric and elastic properties of digital images of random materials. *NISTIR 6269*, U.S. Department of Commerce, December 1998.
18. FEMA 403. World Trade Center building performance study: data collection, preliminary observations, and recommendations. Federal Emergency Management Administration, Washington, DC, May 2002.
19. Standard for Durability Tests for Fire Resistive Materials Applied to Structural Steel, UL 2431, Draft 1.1. Underwriters Laboratories Inc., Northbrook, IL, 2003.
20. Low NMP. Material degradation of thermal insulating mineral fibers. In *Thermal Insulation*: *Materials and Systems*, vol. ASTM STP 922, Powell FJ, Matthews SL (eds). American Society for Testing and Materials: Philadelphia, 1987; 477–492.